

## Infrared Characterization of the Guanine Radical Cation: Finger Printing DNA Damage

Anthony W. Parker,<sup>\*,†</sup> Ching Yeh Lin,<sup>\*,‡</sup> Michael W. George,<sup>§</sup> Michael Towrie,<sup>†</sup> and Marina K. Kuimova<sup>\*,§,||</sup>

Central Laser Facility, Science and Technology Facilities Council, Rutherford Appleton Laboratory, Harwell Science and Innovation Campus, Didcot, Oxfordshire, OX11 0QX, U.K., Research School of Chemistry, Australian National University, ACT 0200, Australia, School of Chemistry, University of Nottingham, University Park, Nottingham, NG7 2RD, U.K., and Chemistry Department, Imperial College London, Exhibition Road, South Kensington, SW7 2AZ, U.K.

Received: November 10, 2009; Revised Manuscript Received: January 27, 2010

Oxidation of DNA represents a major pathway of genetic mutation. We have applied infrared spectroscopy in 77 K glass with supporting density functional theory (DFT) calculations (EDF1/6-31+G\*) to provide an IR signature of the guanine radical cation  $G^{+\bullet}$ , formed as a result of 193 nm photoionization of DNA. Deprotonation of this species to produce the neutral radical  $G(-H)^{\bullet}$  does not occur in 77 K glass. DFT calculations indicate that the formation of  $G^{+\bullet}$  within the double helix does not significantly perturb the geometry of the G/C pair, even though there is a significant movement of the  $N^1$  proton away from G toward C. However, this is in stark contrast to drastic changes that are expected if full deprotonation of G/C occurs, producing the  $G(-H)^{\bullet}/C$  pair. These results are discussed in light of solution-phase time-resolved IR spectroscopic studies and demonstrate the power of IR to follow dynamics of DNA damage in natural environments.

## Introduction

Charge transfer processes represent one of the simplest chemical reactions to induce DNA damage. The crucial intermediates in many charge transfer processes are radical cations of DNA bases,<sup>1,2</sup> formed by electron loss following photoionization and/or oxidative attack of a nucleobase. Since the ionization potentials of the bases vary, following the order  $G < A < T \approx C$ ,<sup>3</sup> the random ionization of DNA, followed by interbase electron transfer, is expected to eventually end in the formation of the most energetically favorable product, the guanine radical cation,  $G^{+\bullet}$ , and/or the neutral radical  $G(-H)^{\bullet}$  produced by deprotonation of initially formed  $G^{+\bullet}$ .<sup>4,5</sup> The timescale on which this proton loss reaction occurs is a subject of controversy,<sup>6–8</sup> especially since it is known to be affected by pH in a free base G,<sup>6</sup> by pairing to C,<sup>7</sup> or by the nature of neighboring bases on the same strand of DNA.<sup>9</sup> These factors, combined with the presence or absence of charge on G can alter oxidation potentials<sup>10–13</sup> and thus play an important role in determining subsequent reactivity and the fixation of damage via secondary reactions of  $G^{+\bullet}/G(-H)^{\bullet}$ , e.g. forming the key mutagenic product of the oxidation of G, 8-hydroxy-2'-deoxyguanosine.<sup>14</sup>

Density functional theory (DFT) calculations have proved to be an invaluable tool in identifying the transient intermediates produced within DNA by radiation. However, the DFT description alone might be incomplete as it often relies on a series of models and simplifications. Yet these simplifications are not always true to life. The problem has been highlighted recently

by calculations of the ionization potential of the guanine base showing that, unexpectedly, the addition of a sugar moiety has a similarly large effect on the calculated potential as pairing to cytosine.<sup>15</sup> Likewise, it has been recently shown that DFT calculations must take hydration into account to correctly predict the proton transfer in the ionized G/C basepair.<sup>16</sup> Thus, ideally, DFT calculations should be used in conjunction with a spectroscopic approach and serve as an aide in interpretation of experimental spectra.

To date, experimental spectroscopic characterization of the ionization and oxidation intermediates in DNA has been performed using a wide variety of methods including nanosecond UV flash photolysis,<sup>5,17</sup> time-resolved and steady-state EPR measurements<sup>18–22</sup> and picosecond time-resolved infrared spectroscopy (ps-TRIR).<sup>8,23,24</sup> TRIR spectroscopy is a powerful technique for providing both molecule-specific structural information and picosecond time resolution. We have demonstrated that TRIR data on DNA bases are particularly informative when combined with DFT calculations aiding in interpretation of IR spectra of transient intermediates.<sup>23</sup>

Here we monitor 193 nm ionization of DNA in rigid aqueous glasses at 77 K with IR spectroscopy. The key premise of our work is to be able to interpret experimental infrared spectra of guanine ionization as a free base and in the DNA helix based on DFT calculations of its vibrational fingerprint.

## Results and Discussion

We first assessed the applicability of DFT calculations by comparing the experimental FTIR spectra of guanine obtained between  $2 \leq \text{pD} \leq 10$  with calculation results. At  $\text{pH} < 2.4$  guanine adds a proton and at  $\text{pH} > 9.4$  it loses a proton,<sup>6</sup> Scheme 1. It is expected that in a  $D_2O$  solution both amino- and imino-protons of G will be rapidly exchanged for deuterons, Scheme

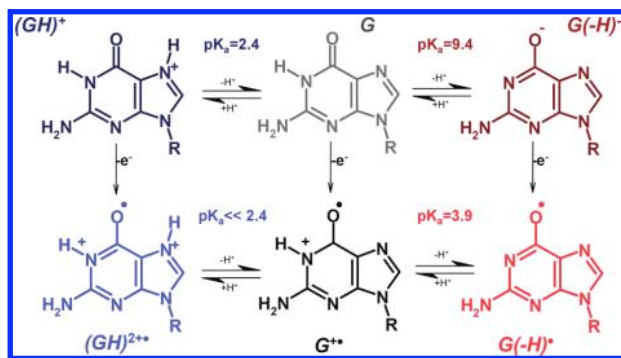
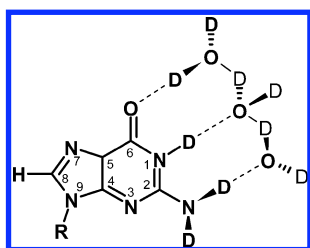
\* To whom correspondence should be addressed. E-mail: (A.W.P.) a.w.parker@stfc.ac.uk; (C.Y.L.) cylin@rsc.anu.edu.au; (M.K.K.) m.kuimova@imperial.ac.uk.

<sup>†</sup> Harwell Science and Innovation Campus.

<sup>‡</sup> Australian National University.

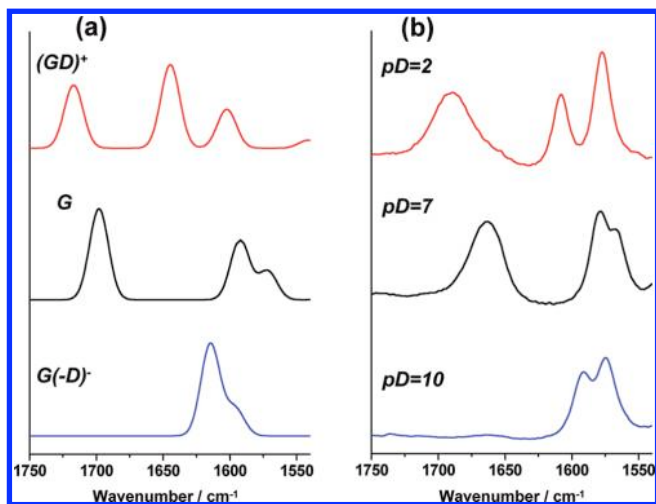
<sup>§</sup> University of Nottingham.

<sup>||</sup> Imperial College London.

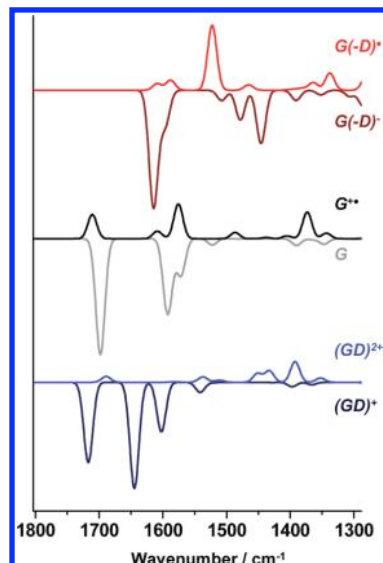
**SCHEME 1: Acid-Base Equilibria for Ground State Guanosine and its Ionization Products in H<sub>2</sub>O**

**SCHEME 2: The Structure of Hydrated Guanine in D<sub>2</sub>O Used for the DFT IR Calculations**


2. Figure 1 compares experimental FTIR spectra of G, (GD)<sup>+</sup> and G(-D)<sup>-</sup> with the calculated spectra of partially deuterated G.

The IR spectra of guanine calculated in the gas phase match with the experimental solution phase FTIR both in relative band positions and intensity (See Figure S2, Supporting Information). Additionally, the shifts of each IR band following protonation/deprotonation are correctly predicted. However, the peak frequencies calculated in the gas phase are overestimated for all species, that is, in the gas phase the bonds responsible for vibrational frequencies between 1500–1700 cm<sup>-1</sup> ( $\nu(\text{C}=\text{O})$  stretching and ND<sub>2</sub> bending) appear at higher frequency than they are in reality. To address this issue and mimic the solvent phase, three hydrogen bonds with D<sub>2</sub>O (see Scheme 2) were used to provide a better representation of the C=O and ND<sub>2</sub> environment in aqueous phase. In this way, we are able to accurately describe both the frequencies of the corresponding



**Figure 1.** Vibrational spectra of guanine protonation/deprotonation products: (GD)<sup>+</sup> (red), G (black), and G(-D)<sup>-</sup> (blue) (a) calculated in solution phase and (b) obtained experimentally.



**Figure 2.** Vibrational spectra calculated in solution phase for (GD)<sup>+</sup>, G(-D)<sup>-</sup> and G and corresponding ionization products. The spectra are color coded according to Scheme 1.

vibrations and the relative band shifts following protonation in the pD range between pD = 2 and pD = 10; see Figure 1a. We have also demonstrated that addition of extra hydrogen bonds with D<sub>2</sub>O molecules (up to 5 D<sub>2</sub>O molecules to fill all the available positions for specific hydrogen bonding with guanine) does not significantly alter calculated IR spectra of guanine; see Figure S3, Supporting Information). Earlier DFT calculations<sup>16</sup> indicate that the number of water molecules used to solvate guanine is an influencing factor for the stability of various ionization products. For example, in the gas phase deprotonated radical G(N2-H)<sup>\*</sup> is more stable than G(N1-H)<sup>\*</sup> by 4.71 kcal/mol; G(N2-H)<sup>\*</sup> is more stable than G(N1-H)<sup>\*</sup> by 2.65 kcal/mol when dGua is associated with one water molecule.<sup>16a</sup> The order of stabilization is reversed with seven water molecules, and G(N1-H)<sup>\*</sup> becomes more stable than G(N2-H)<sup>\*</sup> by 3.26 kcal/mol.<sup>16a</sup> In our calculations, using three D<sub>2</sub>O molecules, we find that G(N1-D)<sup>\*</sup> is more stable than G(N2-D)<sup>\*</sup> (syn conformer) by 4.19 kcal/mol; see Table S1, Supporting Information. This is consistent with the data reported in ref 16a and demonstrates that the model in which only three D<sub>2</sub>O molecules are considered adequately describes the structure of solvated guanine and its ionization products.

Close correlation of calculated IR spectra with experiment, Figure 1b, and the fact that the calculated structures of ionized intermediates are consistent with the literature data (Table S1, Supporting Information) gives confidence that our model of solvation of guanine and the level of theory used are sufficient to describe the FTIR spectra of G and its ionization products at different pH.

Nominally the ejection of an electron from G, (GD)<sup>+</sup>, and G(-D)<sup>-</sup> will form G<sup>+</sup>, (GD)<sup>2++</sup> and G(-D)<sup>\*</sup>, respectively, Scheme 1. The spectra calculated for these ionization products are shown in Figure 2. The calculated IR spectra of the solvated ground state forms of guanine are also shown in Figure 2 as negative bands, next to the bands of the corresponding ionization product. This representation of the calculated spectra offers an easy comparison with our experimental observations. That is, in our photoionization experiments the IR bands of the non-ionized forms of G appear as negative (due to the population decrease of the ground state species) and the bands for the newly formed products appear positive; see Experimental Section for further details.

The direct products of ionization might be unstable in fluid solution, according to Scheme 1. For example, in solution at  $\text{pH} > 3.9$ ,  $\text{G}^{++}$  will ultimately lose a proton to form  $\text{G}(-\text{H})^{\cdot}$ ,<sup>6</sup> since the  $\text{p}K_{\text{a}}$  of  $\text{G}^{++}$  ( $\text{p}K_{\text{a}} = 3.9$ ) is lower than that of  $\text{G}$  ( $\text{p}K_{\text{a}} = 9.4$ ). Thus the nature of the ionization product detected depends on thermodynamic factors (solution pH) as well as kinetic factors (time delay between ionization and observation).

Previously, we have used ps-TRIR to detect guanine ionization products in solution between 2 ps and 2 ns.<sup>8</sup> In our present work, we utilize the fact that in glasses at cryogenic temperatures the transient species formed are extremely stable. This stability has been extensively used in DNA radiation chemistry to study ionization using EPR spectroscopy.<sup>18,19,22</sup> It is thus expected that following ionization of  $\text{G}$  and DNA at 77 K,  $\text{G}^{++}$  is sufficiently stabilized to be detectable spectroscopically.<sup>18</sup> The EPR studies of direct DNA ionization to date have been unable to give conclusive evidence to distinguish between initially formed  $\text{G}^{++}$  and deprotonated  $\text{G}(-\text{H})^{\cdot}$  for either individual  $\text{G}$  or  $\text{G}$  within a DNA helix. Additionally, the solvated electron was not detected<sup>18</sup> in these studies.

A recent EPR study of one-electron oxidized ( $\gamma$ -irradiated) guanine in DNA performed at 77 K has identified that the proton in  $\text{G}^{++}/\text{C}$  pair migrates from  $\text{G}$  to  $\text{C}$ , essentially producing deprotonated  $\text{G}(-\text{H})^{\cdot}$ .<sup>22</sup> We are interested in reproducing this result in “ionized” DNA using IR spectroscopy for identifying the marker bands for all possible ionization products, including fully deprotonated  $\text{G}(-\text{H})^{\cdot}/\text{C}$  pair, where the proton is not merely moved to an adjacent cytosine, but completely lost. These marker bands can be used in the analysis of the ps-TRIR data in fluid solution, such as in ref 8, to monitor the fate of the initially produced ionized/oxidized lesion to the point of fixation of the damage. Establishing IR signatures of ionized bases is important because TRIR represents a unique way to directly monitor the dynamics of formation of  $\text{G}^{++}$  in solution on ultrafast timescales, as well as to follow its subsequent reactions into the microsecond (and beyond) timescale. TRIR is also extremely sensitive to the microenvironment of the bases, that is, neighboring bases, secondary, and tertiary structure.<sup>25,26</sup> Here, we calculate and monitor experimentally IR signatures of guanine ionization both as a free base and in a double helix.

Irradiation of  $\text{G}$  with 193 nm light leads to its ionization.<sup>5,17</sup> Experimental IR spectra obtained following 193 nm irradiation of  $\text{G}$  in a rigid matrix at 77 K are shown in Figure 3b. Note that the experimental results are obtained as difference spectra, final state (post irradiation) minus initial state (prior to irradiation). The detailed description is given in Experimental Section.

The set of Lorentzian bands used to fit the ionization spectrum of  $\text{G}$  is shown in Figure 3c. The fitted bands from the  $\text{pD} = 7$  experiment compare well with the calculated spectra, given in Figure 2b, showing both  $\text{G}$  (negative bands) and  $\text{G}^{++}$  (positive bands). We therefore conclude that  $\text{G}^{++}$  is formed following ionization of  $\text{G}$  at  $\text{pD} = 7$ . To corroborate this conclusion we directly compared both the calculated and experimental findings in Figure 3a,b. It is clear that the calculated and experimental spectra are in good agreement (compare the red lines in Figure 3 panels a and b), and on the basis of this similarity we assign the species formed during photoionization to  $\text{G}^{++}$ .

Further experiments have identified that variation of the  $\text{pD}$  in glass permits additional control of the ionization product states of  $\text{G}$ , consistent with Scheme 1. At  $\text{pD} = 2$ , guanine is present in the form  $(\text{GD})^+$  and its direct ionization should produce  $(\text{GD})^{2++}$ , Scheme 1. The experimental difference IR spectrum of the ionization of  $(\text{GD})^+$  at  $\text{pD} = 2$ , together with the multicurve Lorentzian fit is given in Figure 4. This spectrum

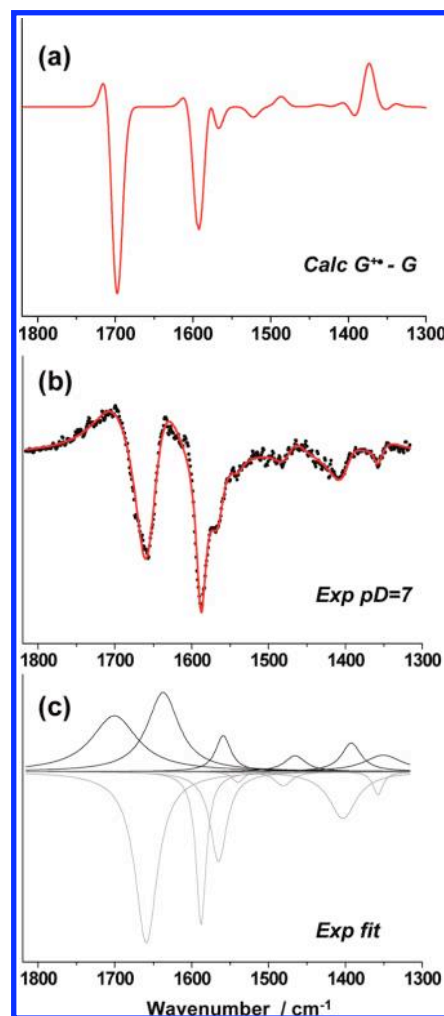


**Figure 3.** (a) A calculated ionization spectrum obtained by subtraction of the spectrum of  $\text{G}$  from the spectrum of  $\text{G}^{++}$ , original spectra are shown in Figure 2b; (b) experimental difference IR spectrum (black) obtained in  $\text{NaClO}_4$  aqueous glass at 77 K following 193 nm ionization of  $\text{G}$  at  $\text{pD} = 7$  with the fit (red), composed of individual Lorentzian bands shown in (c). Bands used to fit the ground state features in the spectrum are shown in gray and the features due to ionized species in black.

shows some differences from the spectrum obtained at  $\text{pD} = 7$  (Figure 3b), mainly evident in the  $1600\text{--}1400\text{ cm}^{-1}$  spectral region as appearance of several additional transient bands. These additional Lorentzian bands, which are not observed in the  $\text{pD} = 7$  spectrum, are shown in blue in Figure 4c. Overall the new bands produced following ionization at  $\text{pD} = 2$  can be well described as a superposition of  $\text{G}^{++}$  and  $(\text{GD})^{2++}$  bands; see Figure 4c. Therefore, at  $\text{pD} = 2$  initially produced  $(\text{GD})^{2++}$  deprotonates to form  $\text{G}^{++}$ , even in 77 K glass. To corroborate this point, the calculated bands for both  $\text{G}^{++}$  and  $(\text{GD})^{2++}$  are given in Figure 4a. Although the  $\text{p}K_{\text{a}}$  value of  $(\text{GD})^{2++}$  has not been reported, we expect it to be less than 2.4, the  $\text{p}K_{\text{a}}$  of corresponding species prior to electron ejection,  $(\text{GD})^+$ ,<sup>6</sup> and therefore it is likely that initially formed  $(\text{GD})^{2++}$  can deprotonate to form  $\text{G}^{++}$ , even in 77 K glass.

It is important that the calculated spectrum of deprotonated species,  $\text{G}(-\text{D})^{\cdot}$ , Figure 2a (red), is very different to that obtained following ionization at either  $\text{pD} = 7$  or  $\text{pD} = 2$ . Specifically, the most characteristic IR band at  $1710\text{ cm}^{-1}$ , predicted by DFT for  $\text{G}^{++}$ , which is shifted to higher wavenumber relative to ground state  $\nu(\text{C}=\text{O})$  in guanine, is present

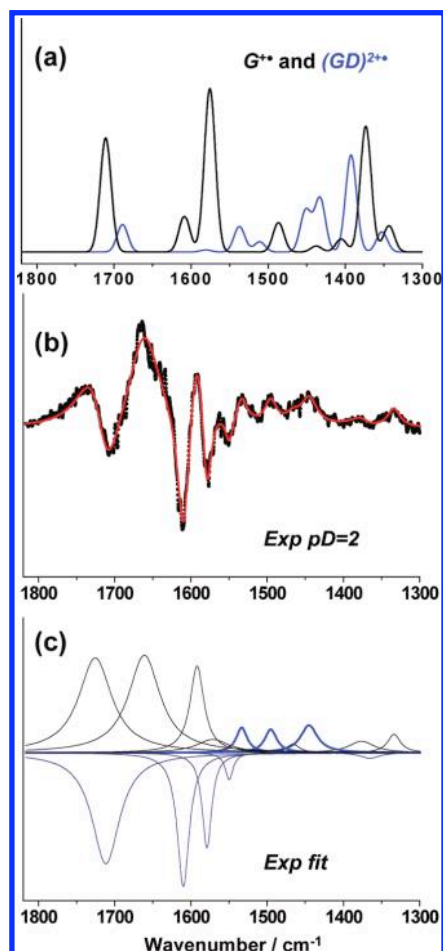


**Figure 4.** (a) The calculated solution phase spectra of  $G^{+}$  and  $(GD)^{2+}$ ; (b) experimental difference IR spectrum (black) obtained in  $\text{NaClO}_4$  aqueous glasses at 77 K following 193 nm ionization of  $(GD)^+$  at  $\text{pD} = 2$  with the fit (red), composed of individual Lorentzian bands shown in (c). Bands used to fit the ground state features in the spectrum are shown in navy and the features due to ionized species in black and blue. We tentatively assign the black-colored positive bands to  $G^{+}$  and the blue-colored positive bands to  $(GD)^{2+}$ .

in the experimental spectrum at  $\text{pD} = 7$  but is absent from the calculated spectrum of  $G(-D)^{\cdot}$ .

Therefore the IR data unequivocally demonstrated that  $G^{+}$  is the major detectable product of photoionization of guanine at 77 K at  $\text{pD} = 7$  and  $G^{+}$  does not significantly deprotonate under these conditions. However, we cannot exclude that deprotonated guanine radical is present in small quantities, since the IR bands for these species are found in the same spectral region as the bands of guanine radical cation, Figure 2. The strongest marker band for  $G(-D)^{\cdot}$  lies at ca.  $1530 \text{ cm}^{-1}$  (Figure 2, red line) and we do not observe this characteristic feature in the experimental spectrum recorded at  $\text{pD} = 7$ . It has been previously concluded on the basis of EPR spectroscopic data in 7.5 M LiCl aqueous glass that significant quantities of deprotonated guanine radical are formed at  $\text{pH} = 7$  following oxidation of guanine,<sup>16a</sup> however our present data do not support this conclusion. The major contributing factor could be the differences in how the radical cation was prepared in each study. In ref 16a, the radical cation was prepared by  $\gamma$ -irradiation followed by annealing at 150 K in a bimolecular reaction with thus generated  $\text{Cl}_2^{\cdot-}$ . In our work, the radical cation was generated directly by 193 nm photoionization at 77 K. Since no annealing was necessary in our work, the initially formed guanine radical cation is more likely to survive at our experimental conditions.

The spectra calculated for ionized intermediates of G in the gas phase (Figure S2, Supporting Information) do not satisfactorily describe the experimental IR spectra of ionized products of G, since they do not take into account the hydrogen bonding interactions with the surrounding  $\text{D}_2\text{O}$ .

We have previously reported the ps-TRIR spectra of photoionized G in solution where we observe a transient band at  $1702 \text{ cm}^{-1}$ , showing a shift to higher energy relative to the parent  $\nu(\text{C}=\text{O})$  band of guanine at  $1662 \text{ cm}^{-1}$ .<sup>8</sup> The assignment of these species to either  $G^{+}$  or  $G(-D)^{\cdot}$  was not clear at that time. On the basis of our present DFT and experimental ionization results at 77 K we can assign the previously observed  $1702 \text{ cm}^{-1}$  band to  $G^{+}$ . This result supports the deprotonation rates reported for this species in a pulse radiolysis study.<sup>7</sup>

Our major goal here is to identify the products resulting from photoionization of G in DNA and assign their IR signatures. This will provide the much needed information to further develop TRIR as an analytical tool capable of following the dynamics of the primary chemical processes in DNA that lead to genetic mutation.

We therefore turn to study the ionization of a synthetic double helical DNA containing only G and C, poly(dGdC)·poly(dGdC). The experimental spectrum obtained following 193 nm irradiation at 77 K is shown in Figure 5a together with individual Lorentzian band fitting, Figure 5b. The assignment of these bands will be discussed below.

The calculated ground state IR spectrum of G/C pair (gas phase) gives good correlation to the experimental IR spectrum of poly(dGdC)·poly(dGdC) in 77 K glass. Since we are using  $\text{D}_2\text{O}$  as solvent, it is expected that all five hydrogen atoms in G/C pair will be replaced by deuterium due to base flipping occurring on the millisecond timescale.<sup>27,28</sup> We will therefore discuss the calculated spectra of deuterated G/C pair in this work.

The calculated IR spectra and the corresponding structures of G/C ionization are shown in Figures 6–8. First, we are interested in comparing our IR results with the findings of the recent EPR study of  $\gamma$ -irradiated guanine in DNA at 77 K, which concluded that the proton in  $G^{+}/C$  pair migrates from G to C, essentially producing deprotonated  $G(-H)^{\cdot}$ .<sup>22</sup> Second, we set out to identify the marker fingerprint bands for alternative ionization products, which could form in 77 K  $\text{D}_2\text{O}$  glass, namely the fully deprotonated  $G(-D)^{\cdot}/C$  pair, where the proton is not merely moved to an adjacent cytosine, but completely lost. Using these IR marker bands we would be able to assign the experimentally observed spectrum of poly(dGdC)·poly(dGdC) both in solution<sup>8</sup> and in 77 K glass (this work) to one of the ionization products.

The IR spectra of  $(G^{+}/C)$  pair directly produced by ionization with varying the degree of imine deuteron transfer from G to C are shown in Figure 6. Calculations were performed by changing the bond length between D (guanine) and  $\text{N}_3$  (cytosine) from 1.84 Å in the structure corresponding to the minimal energy to 1.10 Å, corresponding to complete deuteron transfer to C, in incremental steps of 0.1 Å, while optimizing the geometry of the  $(G^{+}/C)$  pair. The structures of the initial and final states of  $(G^{+}/C)$  during this deuteron transfer are given in Figure 7.

The main bond length changes associated with the deuteron transfer may be seen from Figure 7 and the full list of bond length changes is given in Tables S2, S3 and Figure S5, Supporting Information. The most drastic changes occur in the two adjacent hydrogen bonds across the double helix, namely shortening by 0.25 Å of the  $\text{C}^6=\text{O}$  (guanine)... $\text{NH}_2$  (cytosine) and lengthening by 0.24 Å of the  $\text{NH}_2$  (guanine)... $\text{C}^2=\text{O}$  (cytosine). The  $\text{N}^1\text{H}$  (guanine)... $\text{N}^3$  (cytosine) bond (the direction

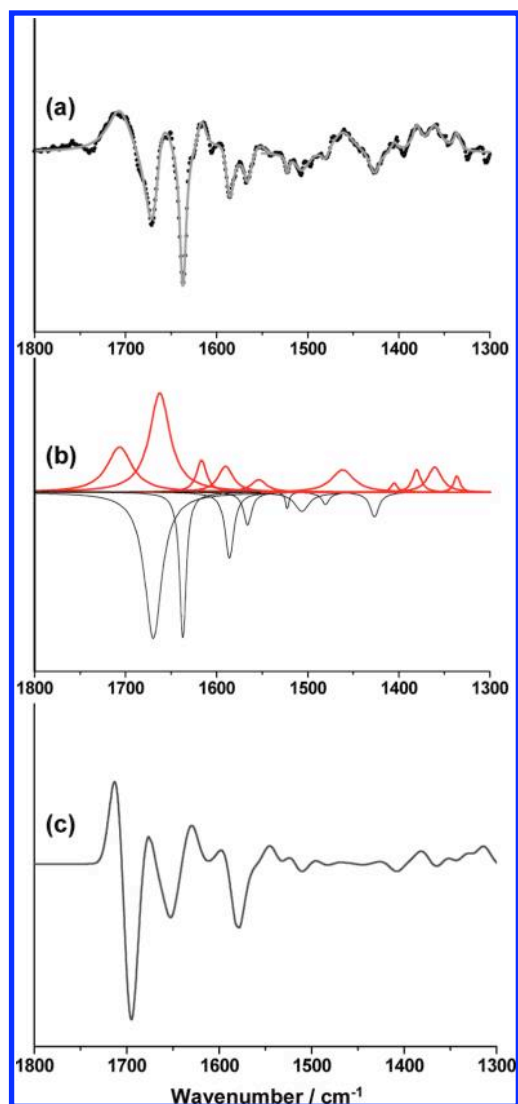


**Figure 5.** (a) Experimental difference IR spectrum (black) obtained in  $\text{NaClO}_4$  aqueous glass at 77 K following 193 nm ionization of poly(dGdC)·poly(dGdC) with the fit (gray); (b) individual Lorentzian bands used to fit the ground state features in the spectrum (black) and the features due to ionized species (red); (c) calculated ionization spectrum of deuterated G/C pair, produced as a sum of individual spectra in Figure 8a,b, corresponding to the ground state G/C and ionized  $\text{G}^+/\text{C}$  with  $\text{N}^1\text{D}(\text{gua})\dots\text{N}^3(\text{cyto})$  distance of 1.2 Å.

of imino proton transfer) is shortened only by 0.02 Å in the geometry-optimized structure after the deuteron transfer.

As expected, the changes in the geometry of ( $\text{G}^+/\text{C}$ ) directly correlate to the changes in frequencies of IR bands; see Figure 6. In particular, the frequencies of  $\nu(\text{CO})$  stretches are affected, due to the change in the strength of the corresponding Watson–Crick hydrogen bonds. Since the highest energy peak in the fingerprint region of the IR spectrum of ( $\text{G}^+/\text{C}$ ) is due to the  $\nu(\text{CO})$  stretch, these geometry changes should be easy to detect by direct comparison with the experimental spectra.

The striking feature of the experimental ( $\text{G}^+/\text{C}$ ) spectrum, Figure 5b (red), is the large positive shift of the high energy  $\nu(\text{CO})$  band compared to that observed in the ground state (black), from 1685 to 1706  $\text{cm}^{-1}$  (21  $\text{cm}^{-1}$ ). This shift is similar to the case of ionization of the free base G (40  $\text{cm}^{-1}$ ), 1662→1702  $\text{cm}^{-1}$  in solution<sup>8</sup> and 1660→1700  $\text{cm}^{-1}$  in 77 K glass (this work). According to our calculations, to reproduce this positive shift in the calculated spectra requires a large shift of imino deuteron from G to C, Figure 6. This result not only

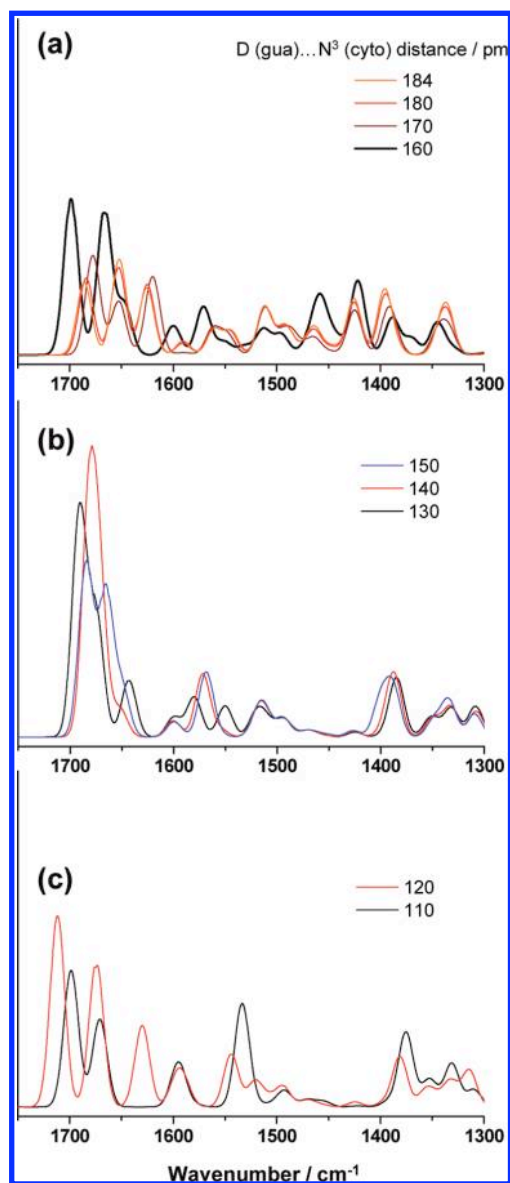


**Figure 6.** The IR spectra of ( $\text{G}^+/\text{C}$ ) pair with varying degree of imine deuteron transfer from G to C by changing the  $\text{D}(\text{gua})\dots\text{N}^3(\text{cyto})$  distance from 1.84 Å (corresponding to the minimal energy) to 1.10 Å (corresponding to a complete deuteron transfer to C). The geometry-optimized structures of the initial and final states of ( $\text{G}^+/\text{C}$ ) during this transfer are given in Figure 7.

confirms recent findings of the EPR study<sup>22</sup> but demonstrates the unique capability of IR spectroscopy to observe the overall changes throughout the complex molecular framework. Comparing experimental data with calculated spectra, we find that the best match, both in band positions and intensity, appears to be the spectrum where the  $\text{D}(\text{guanine})\dots\text{N}^3(\text{cytosine})$  bond is 1.2 Å, Figure 6c; see Figure S6 in Supporting Information for direct comparison. We note that at this distance (<1.4 Å) the deuterium atom is completely transferred from G to C; see Figure S4, Supporting Information. The calculated ionization spectrum of deuterated G/C pair produced as a sum of the ground state IR spectrum of G/C and IR spectrum of  $\text{G}^+/\text{C}$  with  $\text{N}^1\text{D}(\text{gua})\dots\text{N}^3(\text{cyto})$  distance of 1.2 Å is shown in Figure 5c, where it can be directly compared with the experimental spectrum. It is clear that these spectra show remarkable similarity.

A careful inspection of calculated IR spectra of ( $\text{G}^+/\text{C}$ ), Figure 6, reveals that the frequencies of the main IR bands do

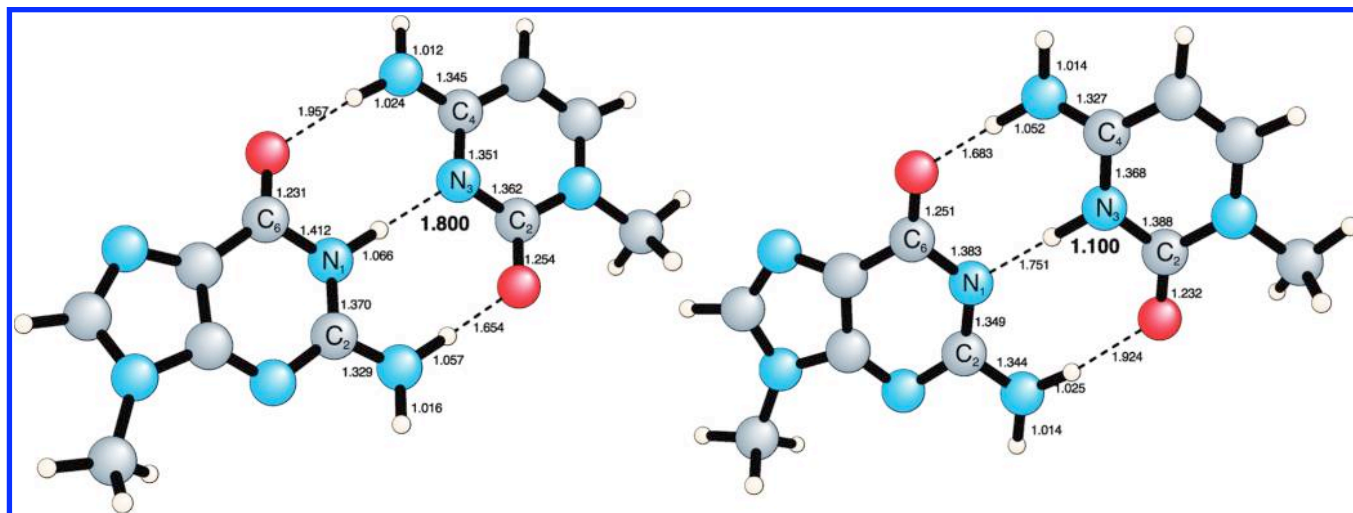


**Figure 7.** The geometry-optimized structures of the initial and final states of  $(G^{+}/C)$  during the imino deuteron transfer from  $N^1D$  (gua) to  $N^3$  (cyto).

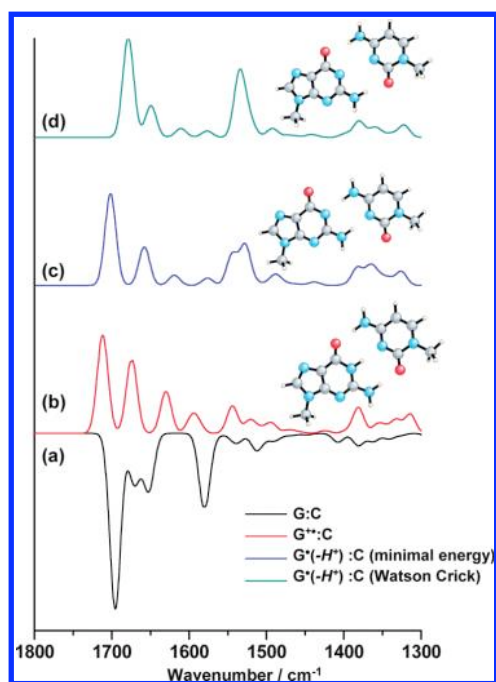


**Figure 8.** IR spectra calculated for deuterated  $G/C$  (a) in the ground state and its ionization products (b)  $G^{+}/C$  with  $N^1D$  (gua)... $N^3$  (cyto) distance of 1.2 Å; (c) deprotonated  $G(-D)/C$  with the shifted hydrogen bond pattern corresponding to a minimal energy and (d) in a Watson–Crick geometry. The geometries of ionized products are shown.

not change smoothly following the shortening of the distance between the imino-deuteron (guanine) and  $N^3$  (cytosine) from 1.84 to 1.1 Å. Indeed there appears to be a drastic change in the spectra, which we will call a “transition state”, occurring at ca. 1.3–1.5 Å between D (guanine)... $N^3$  (cytosine), Figure 6b. Further shortening of this bond leads to a restoration in the overall spectral profile; see Figure 6a,c. The transition state must appear because in the course of deuteron movement from G to C it reaches the state where it is not able to efficiently interact (through either covalent or hydrogen bond) to either G or C. This hypothesis is further discussed below.

We have also calculated the IR spectra of fully deprotonated  $G(-D)/C$  where the deuteron is not merely shifted from G to C, but entirely removed from the base-pair (Figure 8c,d). Interestingly, our DFT calculations suggest that upon complete

deuteron loss from the  $N^1$  position of guanine, forming  $G(-D)/C$ , a marked geometry change takes place (Figure 8c). Specifically, DFT calculations indicate that the most energetically stable conformation of  $G(-D)/C$  is that with a shifted hydrogen bond pattern (Figure 8c) and not the Watson–Crick conformation (Figure 8d). The energy gain from such a shift in the hydrogen bonding pattern is 28 kcal/mol, Table S1, Supporting Information. It is unclear, however, whether such drastic changes can indeed happen in a structurally restrained DNA helix. It is important, however, that the calculated IR spectra of deprotonated  $G(-D)/C$  pair in both conformations do not have the  $\nu(C=O)$  band in the 1700  $cm^{-1}$  region, and this confirms that neither of these species were observed experimentally following 193 nm ionization in 77 K glass (this work) or in solution on the 2 ps to 2 ns timescale.<sup>8</sup> TRIR studies in solution on longer timescales (work in progress) should be able to determine which deprotonated species is formed in the DNA double helix.

It is important that the spectrum of deprotonated  $G(-D)/C$  in the Watson–Crick conformation, Figure 8d bears remarkable similarity to the spectrum of the transition state calculated for  $G^{+}/C$  during the imino deuteron transfer between G and C at ca. 1.4 Å (Figure 6b). This further confirms our earlier conclusion that in this transition state structure the imino deuteron is not able to interact with either G or C and so the transition state resembles fully deprotonated  $G(-D)/C$  pair.

Finally, we have examined the IR spectra of ionized natural Calf Thymus (CT) DNA, which contains all the four nucleobases, G, C, A, and T (Figure S7, Supporting Information). The transient bands obtained following ionization of CT DNA strongly resemble those obtained for poly(dGdC)•poly(dGdC), although the signal recorded is much weaker. Because of this poor signal-to-noise ratio, we cannot rule out the presence of the photoionized products of other bases. In any case, the presence of the positively shifted 1705  $cm^{-1}$  IR band clearly demonstrates the formation of  $G^{+}/C$ , consistent with the low ionization potential of G in DNA and preferential location of the hole on this base.

## Conclusions

The insight into the mechanism and rates of  $G^{+}$  formation and consequent reactivity is crucial for our understanding of radiation-induced DNA damage and mutagenesis, as well as fundamental aspects of DNA photophysics, for example, the

nature of the charge-transfer excited state involving the G/C base pair<sup>29</sup> and relaxation processes associated with the rapid proton transfer that serves as a means to chemically stabilize the integrity DNA helix.<sup>30</sup> Here we have reported the IR spectra of free base G and DNA helices, following photoionization at 77 K. We have assigned the IR signatures of the species formed to G<sup>+</sup> (or G<sup>+</sup>/C in DNA) on the basis of DFT calculations of the vibrational fingerprint of these species. We have established that experimental IR spectra correspond to a geometry of G<sup>+</sup>/C where the imine-proton (or deuteron in G/C pair in D<sub>2</sub>O) is significantly shifted toward C along the hydrogen bond. Overall, formation of G<sup>+</sup>/C leads to a minimal structural perturbation of DNA, while deprotonated product G(-D)/C, which was not detected in experimental spectra at 77 K, can cause significant deformation to the double helix, by disrupting the unique geometry of G/C pair. The present work provides a unique tool for monitoring DNA reactions leading to mutation, which involve G<sup>+</sup> and G(-D)\*.

### Experimental Section

**DFT Calculations.** The EDF1/6-31+G\* functional,<sup>31</sup> which has been shown to be accurate for frequency calculations,<sup>32,33</sup> was used for calculating the harmonic vibrational frequencies of guanine, guanine/cytosine base pair, and corresponding ionization products. The calculations were performed using Q-Chem 2.1 software package.<sup>34</sup> The exchange-correlation quadrature was performed using an Euler–Maclaurin–Lebedev grid<sup>35</sup> with 100 radial and 194 angular points on each atom. Each frequency calculation was preceded by a geometry optimization. If not specified, the spectra of the lowest energy tautomers are always shown. For free-base guanine, the vibrational spectra obtained in a gas phase were compared to those where three specific hydrogen bonds with D<sub>2</sub>O molecules were included to account for the solvatochromic shifts in experimental spectra; see Scheme 2.

**Sample Preparation.** D<sub>2</sub>O (99.99%), DCl (25%), NaClO<sub>4</sub>, 2'-deoxyguanosine-5'-monophosphate, Calf Thymus DNA (all Sigma-Aldrich), and lyophilized poly(dGdC)•poly(dGdC) (Amersham Pharmacia Biosciences) were used as received. FTIR measurements were carried out on Nicolet Avatar 360 spectrometer; prior to data acquisition the spectrometer sample compartment was purged with nitrogen gas for at least 15 min until a negligible change in the background spectrum in the water vapor absorption region (1300–1900 cm<sup>-1</sup>) was achieved. pD was adjusted by adding small aliquots of DCl or NaOH (in D<sub>2</sub>O) to the solution of the sample in pure D<sub>2</sub>O. pH was measured on Hanna Instruments pH210 microprocessor pH meter (±0.02 accuracy) and pD was calculated from these values according to eq 1.<sup>36</sup>

$$\text{pD} = \text{pH} + 0.4 \quad (1)$$

**Infrared Spectroscopy of Ionized Products at Matrix Isolation Conditions.** The measurements at 77 K were performed in a home-built low temperature IR cell, see Supporting Information. Because of the high IR absorption of D<sub>2</sub>O and the way it expands when freezing, it was essential to use a 10 μm path length in all measurements to ensure the formation of clear glassy samples. Aqueous solutions of (poly)nucleotides (ca. 50 mM) were prepared containing 8 M NaClO<sub>4</sub> to assist the formation of glass according to refs 18 and 37. The sample volume was typically 30 μL.

Irradiation was achieved using the 193 nm output produced from an ArF excimer laser (Lambda Physik LPX200, 10 ns pulse

widths). Sample irradiation times were 5 min at 10 Hz over the range of 5 to 20 mJ cm<sup>-2</sup> per pulse. To enable accurate determination of the changes in the weak IR fingerprint vibrations of nucleic bases following ionization, the irradiation was carried out in situ, within the FTIR spectrophotometer, to permit a very accurate background measurement prior to irradiation. The absorption of the sample prior to irradiation was used as a background spectrum in all experiments hence the spectra collected during irradiation appear as difference spectra: final state minus initial state. That is, following irradiation, the ground state bands decrease in intensity (and appear as negative bands in the resulting IR spectra), while the new bands due to ionized products appear as positive bands. Thus obtained experimental spectra are called the “difference IR spectra” in this manuscript. Fitting of the IR spectra was performed in ORIGIN 8.0 (OriginLab, Northampton, MA) using the sum of Lorentzian bands.

**Acknowledgment.** M.K.K. is thankful to the EPSRC Life Sciences Interface programme for a personal fellowship. M.W.G. is grateful to the Royal Society for the Wolfson Merit Award. We thank Professor Mark Searle and Dr. Huw Williams for useful discussions and STFC for funding access to the Central Laser Facility.

**Supporting Information Available:** Experimental IR setup details, additional DFT and spectroscopic data. This material is available free of charge via the Internet at <http://pubs.acs.org>.

### References and Notes

- (1) Melvin, T.; Botchway, S. W.; Parker, A. W.; O'Neill, P. *J. Am. Chem. Soc.* **1996**, *118*, 10031–10036.
- (2) Melvin, T.; Plumb, M. A.; Botchway, S. W.; O'Neill, P.; Parker, A. W. *Photochem. Photobiol.* **1995**, *61*, 584–591.
- (3) Orlov, V. M.; Smirnov, A. N.; Varshavsky, Y. M. *Tetrahedron Lett.* **1976**, 4377–4378.
- (4) Melvin, T.; Botchway, S.; Parker, A. W.; O'Neill, P. *J. Chem. Soc., Chem. Commun.* **1995**, 653–654.
- (5) Candeias, L. P.; Steenken, S. *J. Am. Chem. Soc.* **1993**, *115*, 2437–2440.
- (6) Steenken, S. *Chem. Rev.* **1989**, *89*, 503–520.
- (7) Kobayashi, K.; Tagawa, S. *J. Am. Chem. Soc.* **2003**, *125*, 10213–10218.
- (8) Kuimova, M. K.; Cowan, A. J.; Matousek, P.; Parker, A. W.; Sun, X. Z.; Towrie, M.; George, M. W. *Proc. Natl. Acad. Sci. U.S.A.* **2006**, *103*, 2150–2153.
- (9) Kobayashi, K.; Yamagami, R.; Tagawa, S. *J. Phys. Chem. B* **2008**, *112*, 10752–10757.
- (10) Colson, A. O.; Besler, B.; Sevilla, M. D. *J. Phys. Chem.* **1992**, *96*, 9787–9794.
- (11) Hutter, M.; Clark, T. *J. Am. Chem. Soc.* **1996**, *118*, 7574–7577.
- (12) Kawai, K.; Wata, Y.; Hara, M.; Tojo, S.; Majima, T. *J. Am. Chem. Soc.* **2002**, *124*, 3586–3590.
- (13) Caruso, T.; Carotenuto, M.; Vasca, E.; Peluso, A. *J. Am. Chem. Soc.* **2005**, *127*, 15040–15041.
- (14) Shigenaga, M. K.; Gimeno, C. J.; Ames, B. N. *Proc. Natl. Acad. Sci. U.S.A.* **1989**, *86*, 9697–9701.
- (15) (a) Crespo-Hernández, C. E.; Close, D. M.; Gorb, L.; Leszczynski, J. *J. Phys. Chem. B* **2007**, *111*, 5386–5395. (b) Sun, L. X.; Bu, Y. X. *J. Mol. Struct.-Theochem* **2009**, *909*, 25–32.
- (16) (a) Adhikary, A.; Kumar, A.; Becker, D.; Sevilla, M. D. *J. Phys. Chem. B* **2006**, *110*, 24171–24180. (b) Kumar, A.; Sevilla, M. D. *J. Phys. Chem. B* **2009**, *113*, 11359–11361.
- (17) Candeias, L. P.; Steenken, S. *J. Am. Chem. Soc.* **1992**, *114*, 699–704.
- (18) Malone, M. E.; Symons, M. C. R.; Parker, A. W. *Int. J. Radiat. Biol.* **1994**, *66*, 511–515.
- (19) Wang, W. D.; Yan, M. Y.; Becker, D.; Sevilla, M. D. *Radiat. Res.* **1994**, *137*, 2–10.
- (20) Adhikary, A.; Kumar, A.; Khanduri, D.; Sevilla, M. D. *J. Am. Chem. Soc.* **2008**, *130*, 10282–10292.
- (21) Geimer, J.; Brede, O.; Beckert, D. *Chem. Phys. Lett.* **1997**, *276*, 411–417.

- (22) Adhikary, A.; Khanduri, D.; Sevilla, M. D. *J. Am. Chem. Soc.* **2009**, *131*, 8614–8619.
- (23) Kuimova, M. K.; Gill, P. M. W.; Lin, C. Y.; Matousek, P.; Towrie, M.; Sun, X. Z.; George, M. W.; Parker, A. W. *Photochem. Photobiol. Sci.* **2007**, *6*, 949–955.
- (24) Elias, B.; Creely, C.; Doorley, G. W.; Feeney, M. M.; Moucheron, C.; Kirsch-DeMesmaeker, A.; Dyer, J.; Grills, D. C.; George, M. W.; Matousek, P.; Parker, A. W.; Towrie, M.; Kelly, J. M. *Chem.—Eur. J.* **2008**, *14*, 369–375.
- (25) Doorley, G. W.; McGovern, D. A.; George, M. W.; Towrie, M.; Parker, A. W.; Kelly, J. M.; Quinn, S. J. *Angew. Chem., Int. Ed.* **2009**, *48*, 123–127.
- (26) McGovern, D. A.; Quinn, S.; Doorley, G. W.; Whelan, A. M.; Ronayne, K. L.; Towrie, M.; Parker, A. W.; Kelly, J. M. *Chem. Commun.* **2007**, 5158–5160.
- (27) Gueron, M.; Kochoyan, M.; Leroy, J. L. *Nature* **1987**, *328*, 89–92.
- (28) Laigle, A.; Chinsky, L.; Turpin, P. Y.; Jolles, B. *Nucleic Acids Res.* **1989**, *17*, 2493–2502.
- (29) Sobolewski, A. L.; Domcke, W.; Hattig, C. *Proc. Natl. Acad. Sci. U.S.A.* **2005**, *102*, 17903–17906.
- (30) Groenhof, G.; Schafer, L. V.; Boggio-Pasqua, M.; Goette, M.; Grubmuller, H.; Robb, M. A. *J. Am. Chem. Soc.* **2007**, *129*, 6812–6819.
- (31) Adamson, R. D.; Gill, P. M. W.; Pople, J. A. *Chem. Phys. Lett.* **1998**, *284*, 6–11.
- (32) Watson, T. M.; Hirst, J. D. *J. Phys. Chem. A* **2002**, *106*, 7858–7867.
- (33) Phillips, M. A.; Besley, N. A.; Gill, P. M. W.; Moriarty, P. *Phys. Rev. B: Condens. Matter* **2003**, *67*, 035309.
- (34) Kong, J.; White, C. A.; Krylov, A. I.; Sherrill, D.; Adamson, R. D.; Furlani, T. R.; Lee, M. S.; Lee, A. M.; Gwaltney, S. R.; Adams, T. R.; Ochsenfeld, C.; Gilbert, A. T. B.; Kedziora, G. S.; Rassolov, V. A.; Maurice, D. R.; Nair, N.; Shao, Y. H.; Besley, N. A.; Maslen, P. E.; Dombroski, J. P.; Daschel, H.; Zhang, W. M.; Korambath, P. P.; Baker, J.; Byrd, E. F. C.; Van Voorhis, T.; Oumi, M.; Hirata, S.; Hsu, C. P.; Ishikawa, N.; Florian, J.; Warshel, A.; Johnson, B. G.; Gill, P. M. W.; Head-Gordon, M.; Pople, J. A. *J. Comput. Chem.* **2000**, *21*, 1532–1548.
- (35) Lebedev, V. I. *Sib. Math. J.* **1977**, *18*, 99–107.
- (36) Glasoe, P. K.; Long, F. A. *J. Phys. Chem.* **1960**, *64*, 188–190.
- (37) Malone, M. E.; Symons, M. C. R.; Parker, A. W. *J. Chem. Soc., Perkin Trans. 2* **1993**, 2067–2075.

JP9106958